Original Article

Removal of Cephalexin From Aqueous Solutions Using Magnesium Oxide/Granular Activated Carbon Hybrid Photocatalytic Process

Abdolmotaleb Seid-Mohammadi[1], Mina Bahrami[2], Sana Omari[2], Fateme Asadi[*3]

[1]Social Determinants of Health Research Center, Department of Environmental Health Engineering, Hamadan University of Medical Sciences, Hamadan, Iran
[2]Department of Environmental Health Engineering, Hamadan University of Medical Sciences, Hamadan, Iran
[3]Student Research Committee, Department of Environmental Health Engineering, Hamadan University of Medical Sciences, Hamadan, Iran

*Correspondence to
Fateme Asadi, Email: F_asadi56@yahoo.com

Abstract
In the present study, magnesium oxide/granular activated carbon (MgO/GAC) composite as a catalyst was synthesized using the sol-gel method and its catalytic potential was investigated in the presence of ultraviolet (UV) irradiation for the removal of cephalexin (CLX) in a batch mode reactor. Then, the characterization of the MgO/GAC composite was determined by X-ray diffraction (XRD) and scanning electron microscopy (SEM). Next, the effect of operational parameters was evaluated, including the pH of the solution (3-11), the dosage of composite (1-6 g/L), initial CLX concentration (20-100 mg/L), and contact time (10-60 minutes). The maximum CLX degradation with an initial concentration of 20 mg/L was as high as 98% at pH=3, 4 g/L of MgO/GAC composite with UV irradiation within 60-minute contact time. In addition, the removal process of CLX could be described by the pseudo-first-order kinetic. Further, the chemical oxygen demand (COD) and total organic carbon (TOC) removal rate were 78% and, 62.3% in optimum conditions, respectively. The results indicated that the UV/MgO/GAC hybrid photocatalytic process can be considered as an efficient alternative for treating the wastewater containing CLX.
Keywords: Degradation, Ultraviolet, Cephalexin, Magnesium oxide, Granular activated carbon

1. Introduction

The presence of drugs and their products in wastewater is the main recent concern related to environmental hazards (1). Antibiotics, a well-known type of drug, are used in humans for pharmaceutical treatment and microbial contamination prevention (2). In addition, residual antibiotics are identified in groundwater (3), surface water (4), streams (5), sludge (6), soil (7), and sediment (8). Among different antibiotics, cephalexin (CLX), as a famous member of the cephalosporin family, is extensively used to treat bacterial infections from the respiratory tract, middle ear, along with skin and bones. This organic pollutant is treated insufficiently by conventional treatment processes and may have harmful effects on the health and ecosystems (9). Therefore, the removal of antibiotic residues is important and has generated much research interest. Chemical, physical and biological methods including chemical oxidation (10), biological treatment (11), and physical techniques (12) are used for the removal of antibiotics from the aqueous

environment. However, it is necessary to develop new methods for the effective removal of antibiotics due to the low efficiencies of the above-mentioned methods and the inability of their use. Advanced oxidation processes (AOPs) are widely used for the removal of the antibiotic compounds in aquatic systems. In recent years, different AOPs such as Fenton and Photo-Fenton (13), ozone oxidation (14), sonolysis (15), and photocatalytic oxidation (16) have been applied for degrading a majority of antibiotic compounds in polluted water. Photo-based AOP is an oxidation technology that introduces ultraviolet (UV) irradiation to assist the production and use of free radicals as strong and non-selective oxidants (17). The use of UV irradiation, along with oxidants including hydrogen peroxide (18), ozone (19), and persulfate (20) could be effective for improving the function of oxidation processes. Previous research has evaluated the photodegradation of antibiotics by direct absorption of UV irradiation (21) and combined UV/hydrogen peroxide, UV/periodate, and the like (22). Recently, the

application of the photocatalytic process, in which a catalyst is exposed to UV irradiation to generate hydroxyl radicals (OHᵒ), has been widely considered due to its cost-effectiveness and high efficiency (23). A photocatalyst is a material that improves the chemical reaction rate via adsorbing light to bring it to a higher energy level without final consumption (23). In addition, magnesium oxide (MgO) semiconductors are an important type of metal oxide that can be used as photocatalytic agents in AOPs because of their non-toxicity, unique chemical, mechanical, electronic and optical properties, stability, wide energy band gap, and cost effective (24). MgO can be excited by UV irradiation, resulting in the transition of the electron from the valence band to the conduction band and the formation of holes (MgO_{surf} h^+) and free electrons (MgO_{surf} e^-) on the surface of MgO. MgO_{surf} h^+ with high oxidative ability leads to the direct oxidation of organic contaminants. Hence, nonselective and highly reactive radicals such as hydroxyl radicals are formed by the reaction of the hole with hydroxyl anions and the decomposition of water, which can attack a wide range of organic and inorganic contaminants by converting them into CO_2 and H_2O (25).

Some studies have used MgO nanoparticle as a catalyst for degrading organic pollutions in photocatalytic processes (26,27). These studies clearly indicated that photocatalytic processes using MgO nanoparticles increased the efficiency of organic pollutants from an aqueous medium. However, the separation and recycling of MgO nanoparticles from the reaction medium are more difficult and expensive, which limits its uses on large-scale applications (28). To resolve the above-mentioned technical challenges regarding the use of MgO powder, granular supporting materials coated with MgO are reported to be a feasible alternative (28). Various materials including zeolites, clay, silica, and activated carbon (AC) are considered as supporting materials (29). Among these materials, granular activated carbon (GAC) is considered for use as the support of MgO due to its unique characteristics such as high specific area, highly developed porous structure, low specific density, and low cost superiority (30). Furthermore, GAC as a supporter could absorb increased contaminates to prevent the shock loads, participate in the radical generation, and decompose excess hydrogen peroxide (31). To the best of our knowledge, no study has focused on the degradation of CLX by MgO/GAC as the catalyst composite in the presence of UV irradiation. Therefore, the current study aimed to assess the efficacy of the UV/MgO/GAC process to remove CLX via batch experiments. Finally, the study evaluated the effect of operational parameters such as the pH of the solution, different dosages of catalyst, and different initial CLX concentration.

2. Materials and Methods

2.1. Chemicals and Reagents

CLX (98%; $C_{16}H_{17}N_3O_4S$) (Fig. 1) and GAC were purchased from Sigma Aldrich (St. Louis, MO, USA) and Mg(NO3)2_6H2O (>99% purity), NaOH, and H_2SO_4 were obtained from Merck Chemical Company (Germany). Further, the other chemicals were of analytical grade and used without further purification. Furthermore, 0.1 M sulfuric acid (H_2SO_4) and 0.1 M sodium hydroxide (NaOH) were applied to adjust the pH of the solutions. Eventually, all solutions were prepared by distilled water from the Water Distillation in Chemistry Laboratory, the School of Public Health.

2.2. Preparation and Characterization of Catalyst

In this study, the sol-gel method was used to prepare the GAC/MgO composite. In this method, 10 g of $Mg(NO_3)_2$_$6H_2O$ was initially dissolved in 500 mL deionized water. After stirring for 15 minutes, 3 mL of NaOH (1 N) was added drop by drop under high stirring, followed by adding 10 g of GAC and further stirring for about 60 minutes. The mesh size of GAC was about 14-18 (1-1.41 mm). The GAC used as the support was pre-washed with deionized water and dried in an oven at 60°C for 6 hours. Then, the suspension was transferred into a

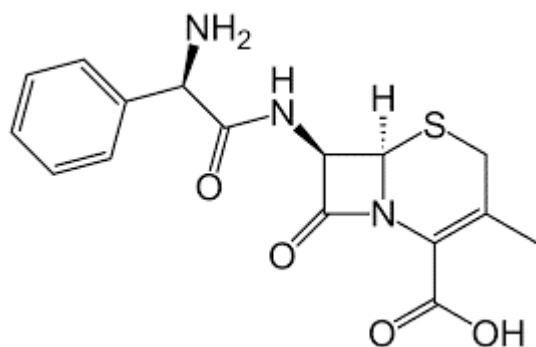**Fig. 1.** Molecular Structure of Cephalexin.

1) Inlet
2) Thermometer
3) UV lamp
4) Quartz Jacket
5) Stainless steel Jacket
6) Photocell
7) Transformator
8) Outlet
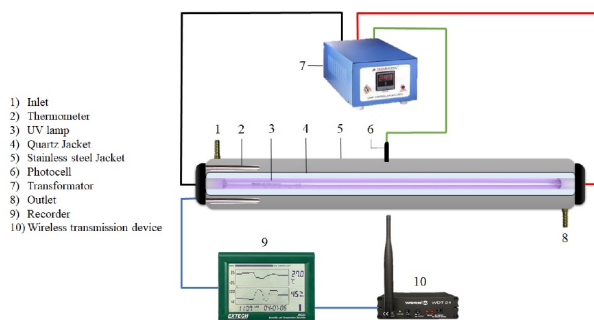9) Recorder
10) Wireless transmission device

Fig. 2. Schematic Diagram of the UV Reactor.

settling beaker and allowed to settle for 60 minutes and the supernatant of the suspension was discharged accordingly. As a result, GAC covering was completed with a white layer of Mg(OH)$_2$ gel on the surface of GAC. Moreover, the Mg(OH)$_2$ covered GAC was dried in an oven at 100°C for 3 hours. Additionally, the calculation process was achieved to convert Mg(OH)$_2$ to MgO nanoparticles in the air at 500°C for 2 hours. The surface morphology of the GAC and GAC/MgO composite was visualized using the scanning electron microscopy (SEM) as well. Finally, the crystal structure of the GAC/MgO composite was analyzed using the X-ray diffraction (XRD) (Bruker-AXS, Germany) by Cu-Kα radiation in the 2θ angles ranging from 20°C to 80°C.

2.3. Photoreactor

All the experiments for CLX removal were carried out using a lab-scale stainless steel photoreactor. A tubular glass photoreactor with a respective total and working volume of 2.5 and 1 L was used to perform the experiments. The UV-C irradiation source for activating MgO/GAC composite was a low-pressure mercury-vapor lamp (55 W, radiation flux for degradation 253.7 nm, Philips Company). Fig. 2 illustrates the graphic representation of the experimental setup.

2.4. Experimental Procedure

In this experimental study, CLX removal was obtained in the batch scale by adding MgO and GAC as a catalyst and a supported catalyst to the synthetic solution, respectively. Briefly, the pH of the CLX sample (1000 mL) was adjusted to the desired level using NaOH and H$_2$SO$_4$ solutions (0.1 mol/L). Then, MgO/GAC composite (1-6 g/L) and CLX (20-100 mg/L) were added to the mixed solution, followed by feeding the solutions into the photoreactor in AOPs. Next, the samples were achieved from the reaction vessel at fixed intervals using a 30

mL syringe and pipetted into glass vials. Eventually, all experiments were repeated twice to reduce the test errors and the averages were reported accordingly.

2.5. Analyses

The samples were taken from the UV reactor at different time intervals and were filtered through a syringe membrane filter (0.2 μm pore size) to remove the MgO particles. Then, the initial and remaining concentrations of CLX were determined, according to (32,33), by spectrophotometry (DR 5000, Hach,). Eight samples were prepared from the stock solutions of CLX in the range of 0.1-10 mg/L to prepare a standard curve (R^2 = 0.9927). A total of 432 samples was tested and all tests were run three times. In addition, all devices were calibrated with a standard solution to ensure reliability across the tests. The efficiency of CLX removal was determined by Eq. (1) as follows:

$$(\%) = (\frac{C_0 - C_t}{C_0}) \times 100 \qquad (1)$$

where %, C$_0$, and C$_t$ represent the percent of CLX removal, initial concentration, and final concentration after different times, respectively (34). Two kinetic models (i.e., first- and second-order types) were used to determine the kinetics coefficients (21).

3. Results and Discussion

3.1. Characterization of Mg/GAC Composite

Figs. 3a and 3b illustrate the results related to SEM micrographs of the surface morphology of GAC and MgO/GAC composite, respectively. As shown, the GAC had an inhomogeneous and granular structure (35) while the MgO/GAC had a flattened surface with heterogeneous small holes. As a result, the surface morphology of the GAC extremely improved after coating with MgO. To investigate the species of coated MgO/GAC, sample of
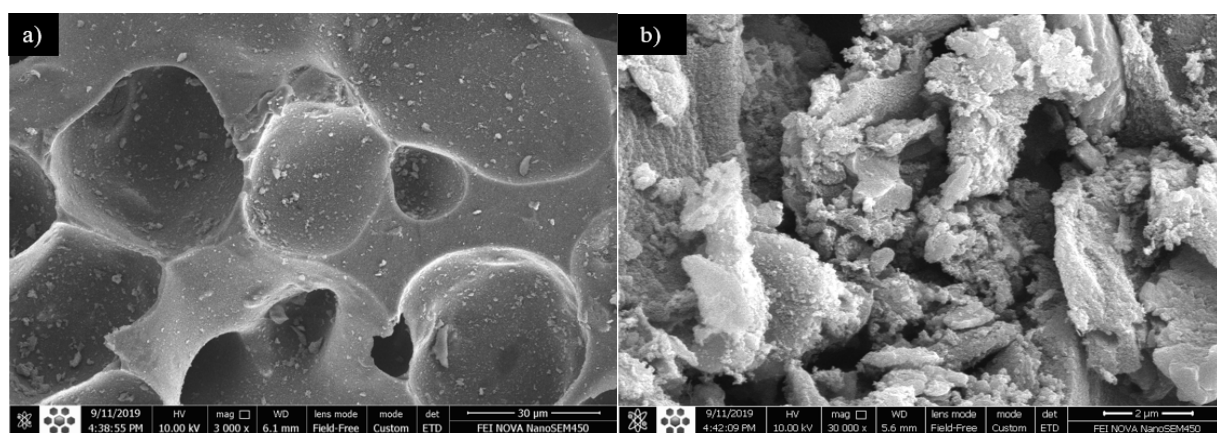

Fig. 3. Scanning Electron Microscopy Image of (a) Granular Activated Carbon GAC Alone and (b) Magnesium Oxide/GAC.
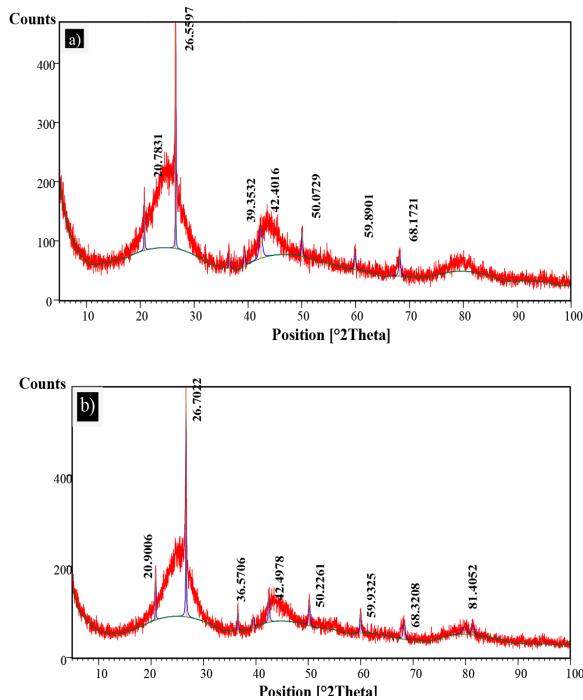
Fig. 4. X-ray Diffraction Pattern of (a) Granular Activated Carbon (GAC) Alone and (b) Magnesium Oxide/GAC.

MgO/GAC was analyzed by X-ray diffraction analyses and compared to GAC. The XRD pattern of GAC and MgO/GAC is depicted in Fig. 4. The peak positions at 43.2°, 50.3°, and 73.8 2θ on the XRD pattern of MgO/GAC are attributed to reflections of MgO and the broad diffraction peak at 43.6° of GAC was attributed to the reflectance. The attendance of MgO in the structure of the MgO/GAC composite achieved the calcination of $Mg(NO_3)_2$ at 500°C on the GAC as the support as well (36).

3.2. Effect of pH

According to Seid-Mohammadi et al (34), the pH of the solution is considered as an effective factor for the removal of organic pollutants using the AOPs. The effect of initial pH on the CLX removal rate in the MgO/GAC/UV system was examined under different pH levels ranging from 3 to 11. The experimental conditions were 20 mg/L CLX, 1.5 mg/L MgO, and 2 g/L GAC at different contact times. The results are displayed in Fig. 5. Based on the results, CLX removal efficiency considerably decreased by increasing the initial pH from 3 to 11 and the CLX removal efficiency was 95%, 73%, 72%, 70%, and 66% at a pH of 3, 5, 7, 9, and 11 within 60-minute contact time, respectively. As shown, the removal of CLX in acidic solution improved, which is in accordance with the results of previous studies (37,38). MgO is excited to produce positive holes in the valence band (hv^+_{vb}) with an oxidative potential, as well as negative electrons at the conduction band (e^-_{cb}) with a reductive potential, as Eq.

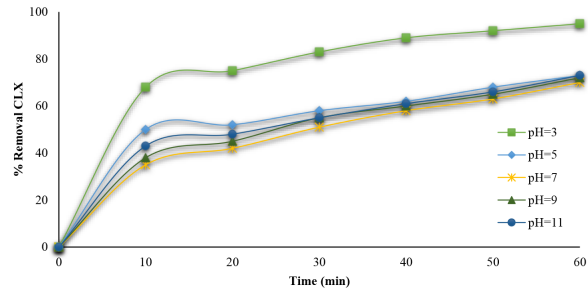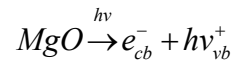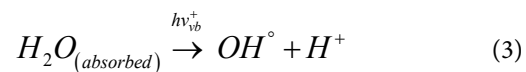**Fig. 5.** Effect of Initial pH on Cephalexin Degradation (CLX=20 mg/L, MgO/GAC=4 g/L)

(1) as follows (39):

$$MgO \xrightarrow{hv} e^-_{cb} + hv^+_{vb}$$

These holes and electrons can generate hydroxyl radicals due to the reactions of OH^-, H_2O, and O_2 at the surface of MgO according to Eqs. (2-4) as follows (40):

$$OH^-_{(surface)} \xrightarrow{hv^+_{vb}} OH^\circ \qquad (2)$$

$$H_2O_{(absorbed)} \xrightarrow{hv^+_{vb}} OH^\circ + H^+ \qquad (3)$$

$$O_{2(absorbed)} \xrightarrow{e^-_{cb}} O_2^{\circ -} \qquad (4)$$

Asgari et al indicated that hydroxyl radical has the highest redox potential in acidic conditions (41). Furthermore, most of the CLX is separated into an ionic form (pKa = 6.88) in acidic conditions, which has most reactivity compared to unseparated CLX (42). Based on the results, when the initial pH was increased, the CLX removal rate gradually decreased as well. This is probably because the MgO ions conversion to Mg^{+2} ions combined with water producing $Mg(OH)_2$ precipitated and settled down reduces the availability of Mg in the solution according to Eq. (5).

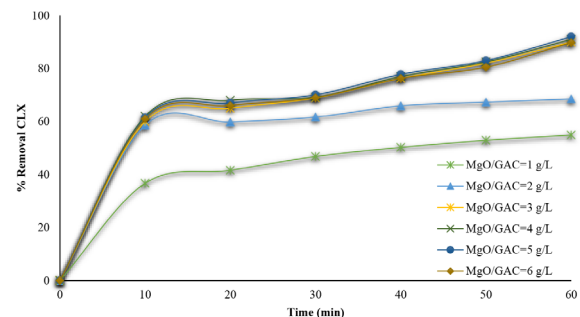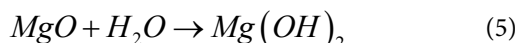**Fig. 6.** Effect of Magnesium Oxide/Granular Activated Carbon Composite Dosage on Cephalexin (CLX) Degradation (pH=3 and CLX=20 mg/L)

$$MgO + H_2O \rightarrow Mg(OH)_2 \qquad (5)$$

In addition, more hydrogen peroxide is decayed without improving the oxidation (43).

3.3. The Effect of MgO/GAC Composite

The effect of the initial dosage of MgO/GAC composite, ranging from 1 to 6 g/L, on CLX removal was investigated and the results are illustrated in Fig. 6. The results showed that the CLX removal efficiency demonstrated an increase from 54.9% to 92% when the dosage of MgO/GAC composite increased from 1 to 4 g/L. This is because the generation of free hydroxyl radicals enhanced by increasing the MgO/GAC composite dosage, which improved the CLX removal rate. Based on previous evidence, MgO is highly reactive with high potential for generating the radicals, which nonselectively attack CLX molecules (28). Although adding an excessive dosage of MgO/GAC composite higher than the optimum dose may decrease the CLX removal efficiency due to the production of Mg^{2+}, it scavenges the generated hydroxyl radicals, leading to a reduction in the CLX removal rate. In addition, several studies reported that the photo sorption of MgO/GAC composite and the number of active sites strongly influence the removal of contaminants. Further, an optimum dosage of MgO/GAC composite
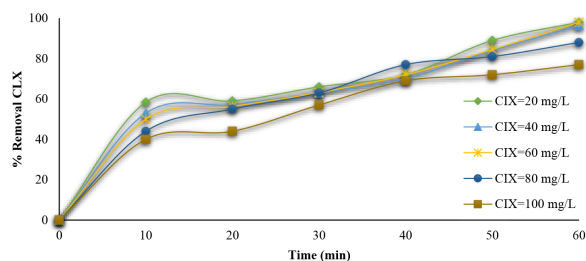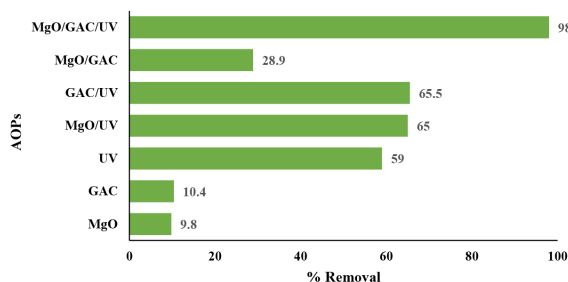
can increase the formation of electron/hole pairs and lead to the production of hydroxyl radicals for enhancing photodegradation. Furthermore, UV penetration reduction due to MgO/GAC composite overdose leads to opacity, which is related to surplus catalyst clusters and thus a simultaneous time increases in the scattering effect (44,45).

3.4. Effect of Initial CLX Concentration

The study further evaluated the effect of the initial CLX concentration ranging from 20 to 100 mg/L on the CLX removal rate, the results of which are depicted in Fig. 7. As shown, the degradation of CLX efficiency decreased when the initial CLX concentration increased to about 100 mg/L. Moreover, the complete degradation of CLX was achieved at 60-minute contact time at a concentration of 20 mg/L CLX solution. Additionally, the removal rate decreased by an increase in the CLX concentration due to a reduction in hydroxyl radical generation (46). This is in line with the results of Moussavi et al (47) and Rivera-Jaimes et al (30).

3.5. The CLX Removal by Different Systems

Fig. 8 displays the comparison of the CLX removal in different systems including MgO, GAC, UV, MgO/UV, GAC/UV, MgO/GAC composite, and MgO/GAC/UV. The experimental conditions were UV irradiation, the CLX of 20 mg/L, a pH of 3, and 60-minute contact time. The results revealed that 1.5 mg/L MgO could achieve a 9.8% CLX removal rate, which was attributed to the limited oxidizing ability of MgO. As shown, the efficiency of CLX removal by the MgO/UV and GAC/UV systems is higher compared to single MgO, GAC, and UV systems. After 60 minutes, the removal of CLX was about 65% and 65.5% for the combined MgO/UV and GAC/UV, respectively. Similarly, the MgO/GAC hybrid had a catalytic efficiency 2.7 times that of GAC alone (Fig. 7), which means that GAC had a lower oxidation rate (28). The related result showed that the CLX removal was refractory to the MgO induced oxygen activation and

Fig. 7. Effect of Initial Cephalexin Concentration on its Degradation   (pH=3 and MgO/GAC=4 g/L).

Fig. 8. Effect of Different Systems on Cephalexin Degradation.
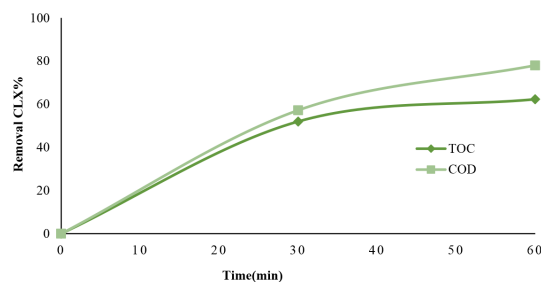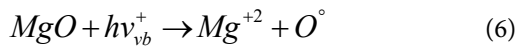

Fig. 9. Chemical Oxygen Demand and Total Organic Carbon Removal Rate in Optimum Conditions (pH=3, MgO/GAC=4 g/L, and CLX=20 mg/L)

the formation of hydroxyl radicals was induced by the activation of MgO using UV irradiation which was not enough to continue the removal of CLX. It was also found that UV irradiation could activate MgO via Eq. (6).

$$MgO + hv_{vb}^{+} \rightarrow Mg^{+2} + O^{\circ} \qquad (6)$$

Likewise, UV irradiation could improve the photocatalytic AOP efficiency due to its ability for generating OH° in the solution (48). Accordingly, the CLX removal rate enhanced up to 95% following adding GAC as catalyst support to the solution with MgO in the presence of the UV irradiation. This phenomenon indicated that a specific and synergistic effect exists between MgO and GAC in the presence of UV irradiation. In addition, the synergistic effect may be defined by UV initiation which increases the mass transfer rate of the system.

3.6. Mineralization of CLX

In this study, the chemical oxygen demand (COD) and total organic carbon (TOC) were investigated to determine the efficiency of CLX removal in MgO/GAC/UV at optimal conditions and the obtained results are illustrated in Fig. 9. The experimental conditions were based on the achieved optimal parameters, including a pH of solution 3, the MgO dosage of 1.5 mg/L, the GAC of 2 g/L, and MgO/GAC composite 4 mg/L at different contact times. Fig. 8 displays that the rates of CLX mineralization regarding COD and TOC removal were 78% and 62.3% after 60-minute contact time, respectively. However, the results showed that the CLX degradation rate was 98% under the same operational conditions, which is extremely higher than the removal rates of COD and TOC since CLX was converted into intermediate metabolites. This finding is in agreement with a report by Rizzo et al. for the removal of diclofenac by using photocatalyst oxidation (49). They reported that the COD removal rate was 85% whereas its removal rate was 94%. These results corroborate the results of Xekoukoulotakis et al (50).
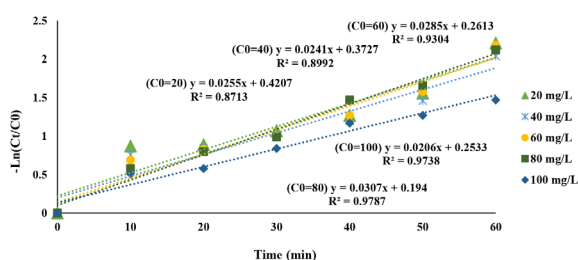
3.7. Kinetic Analysis

Chemical kinetics is applicable for investigating the rate of chemical compound reactions. The rate of a reaction could be expressed by decreasing the concentration of a reactant in reaction time or increasing the concentration of their product per reaction time (34). In this study, the pseudo-first- and second-order kinetics models were applicable for CLX removal and were calculated using Eqs. (6) and (7). Thus, the kinetics of the CLX antibiotic removal was studied in optimum conditions by using the above-mentioned models. The results are presented in Figs. 10 and 11 and Table 1. According to the results, the regression coefficients (R^2) of the kinetic model for the first- and the second-order models were 0.97 and 0.85, respectively. In addition, the pseudo-first-order model was achieved with a considerable coefficient of correlation (R^2) and was the preferable model to fit the data of CLX removal compared to the other kinetics model. The experimental result further indicated that the GAC/MgO composite was an efficient degraded composite for the CLX removal from aqueous solution. The obtained rate constant (k) for CLX antibiotic removal was 0.0255 min^{-1} using the MgO/GAC/UV hybrid process. These results are in conformity with the results of Seid-Mohammadi et al (34), Rocha et al (51), and Samarghandi et al (52).

$$\ln\left(\frac{C_0}{C_t}\right) = -k_1 t \qquad (7)$$

Table 1. Kinetic Parameters of CLX Removal by the MgO/GAC/UV AOPs

C$_0$ (mg/L)	Pseudo-first order		Pseudo-second order	
	K (min^{-1})	R^2	K (L/mg.min)	R^2
C$_0$=20 mg/L	0.03	0.87	0.006	0.75
C$_0$=40 mg/L	0.02	0.90	0.002	0.74
C$_0$=60 mg/L	0.03	0.93	0.002	0.78
C$_0$=80 mg/L	0.03	0.98	0.001	0.92
C$_0$=100 mg/L	0.03	0.97	0.0005	0.85

Note. CLX: Cephalexin; MgO: Magnesium oxide; GAC: Granular activated carbon; UV: Ultraviolet; AOPs: Advanced oxidation processes

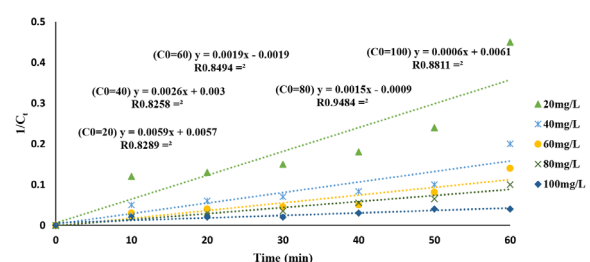**Fig. 10.** Pseudo First-Order Plot for Cephalexin Removal Utilizing the UV/MgO/GAC System.

Fig. 11. Pseudo Second-Order Plot for Cephalexin Removing Using the UV/MgO/GAC System.

$$\frac{1}{C_t} - \frac{1}{C_0} = -Kt$$

(8)

where C_0 and C_t are the initial and final concentrations of CLX an3tibiotic, respectively, and k is a constant of removal value. Finally, *k* value is equal to the slope of the plot of ln (C_0/C_t) versus time *t*.

4. Conclusion

The present study investigated the photocatalytic degradation of CLX antibiotic at different operational parameters using the UV/MgO/GAC system. It was observed that the degradation of CLX was affected by varying the pH range of 3-11. The highest CLX removal rate was achieved at pH=3. In addition, the degradation of CLX was found to increase by increasing the MgO/GAC composite by varying the dosage range of 1-4 g/L while the degradation rate decreased above 4g/L. The experimental results indicated that the CLX removal rate relies on CLX initial concentration and the removal rate decreases by increasing the CLX initial concentration. Under optimal situations, the COD and TOC removal efficiency were obtained to be 78% and 62.3%, respectively. Therefore, the removal process of CLX could be described by pseudo-first-order kinetic. Considering the above-mentioned results, the UV/MgO/GAC system is suggested as an appropriate technique for removing CLX in the wastewater.

Conflict of Interest Disclosures

The authors declare that they have no conflict of interests.

References

1. Harrabi M, Varela Della Giustina S, Aloulou F, Rodriguez-Mozaz S, Barceló D, Elleuch B. Analysis of multiclass antibiotic residues in urban wastewater in Tunisia. Environ Nanotechnol Monit Manag. 2018;10:163-70. doi: 10.1016/j.enmm.2018.05.006.

2. Ong TTX, Blanch EW, Jones OAH. Predicted environmental concentration and fate of the top 10 most dispensed Australian prescription pharmaceuticals. Environ Sci Pollut Res Int. 2018;25(11):10966-76. doi: 10.1007/s11356-018-1343-5.

3. Bexfield LM, Toccalino PL, Belitz K, Foreman WT, Furlong ET. Hormones and pharmaceuticals in groundwater used as a source of drinking water across the United States. Environ Sci Technol. 2019;53(6):2950-60. doi: 10.1021/acs.est.8b05592.

4. Rivera-Jaimes JA, Postigo C, Melgoza-Alemán RM, Aceña J, Barceló D, López de Alda M. Study of pharmaceuticals in surface and wastewater from Cuernavaca, Morelos, Mexico: Occurrence and environmental risk assessment. Sci Total Environ. 2018;613-614:1263-74. doi: 10.1016/j.scitotenv.2017.09.134.

5. Huerta B, Rodriguez-Mozaz S, Lazorchak J, Barcelo D, Batt A, Wathen J, et al. Presence of pharmaceuticals in fish collected from urban rivers in the U.S. EPA 2008-2009 National Rivers and Streams Assessment. Sci Total Environ. 2018;634:542-9. doi: 10.1016/j.scitotenv.2018.03.387.

6. Villar-Navarro E, Baena-Nogueras RM, Paniw M, Perales JA, Lara-Martin PA. Removal of pharmaceuticals in urban wastewater: high rate algae pond (HRAP) based technologies as an alternative to activated sludge based processes. Water Res. 2018;139:19-29. doi: 10.1016/j.watres.2018.03.072.

7. Li Y, Sallach JB, Zhang W, Boyd SA, Li H. Insight into the distribution of pharmaceuticals in soil-water-plant systems. Water Res. 2019;152:38-46. doi: 10.1016/j.watres.2018.12.039.

8. Al-Khazrajy OSA, Bergström E, Boxall ABA. Factors affecting the dissipation of pharmaceuticals in freshwater sediments. Environ Toxicol Chem. 2018;37(3):829-38. doi: 10.1002/etc.4015.

9. Adel AS, Lalung J, Efaq AN, Ismail N. Removal of cephalexin antibiotic and heavy metals from pharmaceutical effluents using Bacillus subtilis strain. Expert Opin Environ Biol. 2015;4(2):1-8. doi: 10.4172/2325-9655.1000117.

10. Ji Y, Fan Y, Liu K, Kong D, Lu J. Thermo activated persulfate oxidation of antibiotic sulfamethoxazole and structurally related compounds. Water Res. 2015;87:1-9. doi: 10.1016/j.watres.2015.09.005.

11. Sui Q, Jiang C, Zhang J, Yu D, Chen M, Wang Y, et al. Does the biological treatment or membrane separation reduce the antibiotic resistance genes from swine wastewater through a sequencing-batch membrane bioreactor treatment process. Environ Int. 2018;118:274-81. doi: 10.1016/j.envint.2018.06.008.

12. Yu F, Li Y, Han S, Ma J. Adsorptive removal of antibiotics from aqueous solution using carbon materials. Chemosphere. 2016;153:365-85. doi: 10.1016/j.chemosphere.2016.03.083.

13. Shemer H, Kunukcu YK, Linden KG. Degradation of the pharmaceutical metronidazole via UV, Fenton and photo-Fenton processes. Chemosphere. 2006;63(2):269-76. doi: 10.1016/j.chemosphere.2005.07.029.

14. Wang L, Li Y, Ben W, Hu J, Cui Z, Qu K, et al. In-situ sludge ozone-reduction process for effective removal of fluoroquinolone antibiotics in wastewater treatment plants. Sep Purif Technol. 2019;213:419-25. doi: 10.1016/j.seppur.2018.12.062.

15. Almasi A, Dargahi A, Mohamadi M, Biglari H, Amirian F, Raei M. Removal of Penicillin G by combination of sonolysis and Photocatalytic (sonophotocatalytic) process from aqueous solution: process optimization using RSM (Response Surface Methodology). Electron Physician. 2016;8(9):2878-87. doi: 10.19082/xx.

16. Karaolia P, Michael-Kordatou I, Hapeshi E, Drosou C, Bertakis Y, Christofilos D, et al. Removal of antibiotics, antibiotic-resistant bacteria and their associated genes by graphene-based TiO2 composite photocatalysts under solar radiation in urban wastewaters. Appl Catal B Environ. 2018;224:810-24. doi: 10.1016/j.apcatb.2017.11.020.

17. Brillas E. A review on the degradation of organic pollutants in waters by UV photoelectro-Fenton and solar photoelectro-Fenton. J Braz Chem Soc. 2014;25(3):393-417. doi: 10.5935/0103-5053.20130257.

18. Rosario-Ortiz FL, Wert EC, Snyder SA. Evaluation of UV/H2O2 treatment for the oxidation of pharmaceuticals in wastewater. Water Res. 2010;44(5):1440-8. doi: 10.1016/j.watres.2009.10.031.

19. Lester Y, Avisar D, Gozlan I, Mamane H. Removal of pharmaceuticals using combination of UV/H(2)

O(2)/O(3) advanced oxidation process. Water Sci Technol. 2011;64(11):2230-8. doi: 10.2166/wst.2011.079.

20. Tan C, Fu D, Gao N, Qin Q, Xu Y, Xiang H. Kinetic degradation of chloramphenicol in water by UV/persulfate system. J Photochem Photobiol A Chem. 2017;332:406-12. doi: 10.1016/j.jphotochem.2016.09.021.

21. Seid-mohammadi A, Amiri R, Faradmal J, Lili M, Asgari G. UVA-LED assisted persulfate/nZVI and hydrogen peroxide/nZVI for degrading 4-chlorophenol in aqueous solutions. Korean J Chem Eng. 2018;35(3):694-701. doi: 10.1007/s11814-017-0317-5.

22. Litter MI. Introduction to photochemical advanced oxidation processes for water treatment. In: Boule P, Bahnemann DW, Robertson PKJ, eds. Environmental photochemistry part II. Berlin, Heidelberg: Springer; 2005. p. 325-66.

23. Toor R, Mohseni M. UV-H2O2 based AOP and its integration with biological activated carbon treatment for DBP reduction in drinking water. Chemosphere. 2007;66(11):2087-95. doi: 10.1016/j.chemosphere.2006.09.043.

24. Moussavi G, Mahmoudi M. Removal of azo and anthraquinone reactive dyes from industrial wastewaters using MgO nanoparticles. J Hazard Mater. 2009;168(2-3):806-12. doi: 10.1016/j.jhazmat.2009.02.097.

25. Hashaikeh R, Szpunar JA. Electrolytic processing of MgO coatings. J Phys Conf Ser. 2009;165(1):012008. doi: 10.1088/1742-6596/165/1/012008.

26. Rezaii Mofrad MR, Mostafaii G, Nemati R, Akbari H, Hakimi N. Removal of methyl orange from synthetic wastewater using nano-MgO and nano-MgO/UV combination. Desalin Water Treat. 2016;57(18):8330-5. doi: 10.1080/19443994.2015.1017744.

27. Talaiekhozani A, Torkan N, Banisharif F, Eskandari Z, Rezania S, Park J, et al. Comparison of Reactive Blue 203 Dye Removal Using Ultraviolet Irradiation, Ferrate (VI) Oxidation Process and MgO Nanoparticles. Avicenna J Environ Health Eng. 2018;5(2):78-90. doi: 10.15171/ajehe.2018.11.

28. Moussavi G, Aghapour AA, Yaghmaeian K. The degradation and mineralization of catechol using ozonation catalyzed with MgO/GAC composite in a fluidized bed reactor. Chem Eng J. 2014;249:302-10. doi: 10.1016/j.cej.2014.03.059.

29. Faria PCC, Órfão JJM, Pereira MFR. Activated carbon and ceria catalysts applied to the catalytic ozonation of dyes and textile effluents. Appl Cata B Environ. 2009;88(3-4):341-50. doi: 10.1016/j.apcatb.2008.11.002.

30. Rivera-Utrilla J, Sánchez-Polo M, Gómez-Serrano V, Alvarez PM, Alvim-Ferraz MC, Dias JM. Activated carbon modifications to enhance its water treatment applications. An overview. J Hazard Mater. 2011;187(1-3):1-23. doi: 10.1016/j.jhazmat.2011.01.033.

31. Guo Q, Liu Y, Qi G, Jiao W. Adsorption and desorption behaviour of toluene on activated carbon in a high gravity rotating bed. Chem Eng Res Des. 2019;143:47-55. doi: 10.1016/j.cherd.2019.01.005.

32. Fazilati M. Photocatalytic degradation of amoxicillin, cephalexin, and tetracycline from aqueous solution: comparison of efficiency in the usage of TiO2, ZnO, or GO-Fe3O4 nanoparticles. Desalin Water Treat. 2019;169:222-31. doi: 10.5004/dwt.2019.24632.

33. Balarak D, Kord Mostafapour F. Photocatalytic degradation of amoxicillin using UV/Synthesized NiO from pharmaceutical wastewater. Indones J Chem. 2019;19(1):211-8. doi: 10.22146/ijc.33837.

34. Seid-Mohammadi A, Asgarai G, Ghorbanian Z, Dargahi A. The removal of cephalexin antibiotic in aqueous solutions by ultrasonic waves/hydrogen peroxide/nickel oxide nanoparticles (US/H2O2/NiO) hybrid process. Sep Sci Technol. 2019:1-11. doi: 10.1080/01496395.2019.1603241.

35. Moussavi G, Rashidi R, Khavanin A. The efficacy of GAC/MgO composite for destructive adsorption of benzene from waste air stream. Chem Eng J. 2013;228:741-7. doi: 10.1016/j.cej.2013.05.032.

36. Richards R, Mulukutla RS, Mishakov I, Chesnokov V, Volodin A, Zaikovski V, et al. Nanocrystalline ultra high surface area magnesium oxide as a selective base catalyst. Scr Mater. 2001;44(8-9):1663-6. doi: 10.1016/S1359-6462(01)00877-6.

37. Davididou K, Monteagudo JM, Chatzisymeon E, Durán A, Expósito AJ. Degradation and mineralization of antipyrine by UV-A LED photo-Fenton reaction intensified by ferrioxalate with addition of persulfate. Sep Purif Technol. 2017;172:227-35. doi: 10.1016/j.seppur.2016.08.021.

38. Zazo JA, Pliego G, García-Muñoz P, Casas JA, Rodriguez JJ. UV-LED assisted catalytic wet peroxide oxidation with a Fe(II)-Fe(III)/activated carbon catalyst. Appl Catal B Environ. 2016;192:350-6. doi: 10.1016/j.apcatb.2016.04.010.

39. Zuorro A, Fidaleo M, Fidaleo M, Lavecchia R. Degradation and antibiotic activity reduction of chloramphenicol in aqueous solution by UV/H2O2 process. J Environ Manage. 2014;133:302-8. doi: 10.1016/j.jenvman.2013.12.012.

40. Deng Y, Zhao R. Advanced Oxidation Processes (AOPs) in Wastewater Treatment. Curr Pollut Rep. 2015;1(3):167-76. doi: 10.1007/s40726-015-0015-z.

41. Asgari G, Seidmohammadi A, Chavoshani A. Pentachlorophenol removal from aqueous solutions by microwave/persulfate and microwave/H2O2: a comparative kinetic study. J Environ Health Sci Eng. 2014;12:94. doi: 10.1186/2052-336x-12-94.

42. Legnoverde MS, Simonetti S, Basaldella EI. Influence of pH on cephalexin adsorption onto SBA-15 mesoporous silica: theoretical and experimental study. Appl Surf Sci. 2014;300:37-42. doi: 10.1016/j.apsusc.2014.01.198.

43. Verma S, Sillanpää M. Degradation of anatoxin-a by UV-C LED and UV-C LED/H2O2 advanced oxidation processes. Chem Eng J. 2015;274:274-81. doi: 10.1016/j.cej.2015.03.128.

44. Yari K, Seidmohammadi A, Khazaei M, Bhatnagar A, Leili M. A comparative study for the removal of imidacloprid insecticide from water by chemical-less UVC, UVC/TiO2 and UVC/ZnO processes. J Environ Health Sci Eng. 2019;17(1):337-51. doi: 10.1007/s40201-019-00352-3.

45. Verma A, Dixit D. Photocatalytic degradability of insecticide chlorpyrifos over UV irradiated titanium dioxide in aqueous phase. Int J Environ Sci. 2012;3(2):743-55.

46. Wu J, Zhang H, Qiu J. Degradation of Acid Orange 7 in aqueous solution by a novel electro/Fe2+/peroxydisulfate process. J Hazard Mater. 2012;215-216:138-45. doi: 10.1016/j.jhazmat.2012.02.047.

47. Moussavi G, khavanin A, Alizadeh R. The integration of ozonation catalyzed with MgO nanocrystals and the biodegradation for the removal of phenol from saline wastewater. Appl Catal B Environ. 2010;97(1-2):160-7. doi: 10.1016/j.apcatb.2010.03.036.

48. Seid-Mohammadi A, Shabanloo A, Fazlzadeh M, Poureshgh Y. Degradation of acid blue 113 by US/H2O2/Fe2+ and US/S2O8 2–/Fe2+ processes from aqueous solutions. Desalin Water Treat. 2017;78:273-80. doi: 10.5004/dwt.2017.20745.

49. Rizzo L, Meric S, Kassinos D, Guida M, Russo F, Belgiorno V. Degradation of diclofenac by TiO2 photocatalysis: UV absorbance kinetics and process evaluation through a set of toxicity bioassays. Water Res. 2009;43(4):979-88. doi: 10.1016/j.watres.2008.11.040.

50. Xekoukoulotakis NP, Xinidis N, Chroni M, Mantzavinos D, Venieri D, Hapeshi E, et al. UV-A/TiO2 photocatalytic decomposition of erythromycin in water: factors affecting mineralization and antibiotic activity. Catal Today. 2010;151(1-2):29-33. doi: 10.1016/j.cattod.2010.01.040.

51. da Rocha ORS, Dantas RF, do Nascimento Júnior WJ, Fujiwara Y, Duarte MMMB, da Silvaa JP. Kinetic study and modelling of cephalexin removal from aqueous solution by advanced oxidation processes through artificial neural networks. Desalin Water Treat. 2017;92:72-9. doi: 10.5004/dwt.2017.21438.

52. Samarghandi MR, Rahmani AR, Samadi MT, Kiamanesh M, Azarian G. Degradation of pentachlorophenol in aqueous solution by the UV/ZrO2/H2O2 photocatalytic process. Avicenna J Environ Health Eng. 2015;2(2):4761. doi: 10.17795/ajehe-4761.